

# Magnetic and superconducting phase diagram of electron-doped $\text{Pr}_{1-x}\text{LaCe}_x\text{CuO}_4$

M. Fujita<sup>1,\*</sup>, T. Kubo<sup>1</sup>, S. Kuroshima<sup>1</sup>, T. Uefuji<sup>1</sup>, K. Kawashima<sup>1</sup>, K. Yamada<sup>1</sup>, I. Watanabe<sup>2</sup>, and K. Nagamine<sup>2,3</sup>

<sup>1</sup>*Institute for Chemical Research, Kyoto University, Uji, Kyoto 610-0011, Japan*

<sup>2</sup>*RIKEN (The Institute of Physical and Chemical Research), Wako, Saitama 351-0198, Japan* and

<sup>3</sup>*Meson Science Laboratory, Institute of Materials Structure Science,*

*High Energy Accelerator Research Organization (KEK-MSL), Tsukuba, Ibaraki 305-0801, Japan*

(Dated: February 20, 2019)

We have investigated the magnetism and the superconductivity of an electron-doped  $\text{Pr}_{1-x}\text{LaCe}_x\text{CuO}_4$  (PLCCO) using single crystal and powder samples by means of zero-field muon spin rotation/relaxation (ZF- $\mu$ SR) and magnetic susceptibility measurements. Muon spin rotation corresponding to antiferromagnetic (AF) order was observed in the sample with  $0.04 \leq x \leq 0.11$ . Changes in magnetic properties of Cu spins upon Ce doping were revealed because the effect of the rare earth moment was negligible. Bulk superconductivity was identified in a wide Ce concentration range of  $0.09 \leq x \leq 0.20$  with a maximum transition temperature of 26 K. At low temperatures, the superconducting (SC) phase abruptly appears by doping with linking quick destroy of the AF ordered phase at  $x \sim 0.09$ , indicating the competitive relation between two phases.

PACS numbers: 74.25.Dw, 74.72.Jt, 75.30.Kz, 76.75.+i

Electron-hole symmetry of a pairing mechanism is one of the central issues in a research on high- $T_c$  superconductivity. It is widely believed that a universal role of magnetism exists because either type of carrier doping into Mott insulators induces superconductivity. Electronic phase diagrams provide important clues for understanding the relationship between magnetism and superconductivity. In the hole-doped  $\text{La}_{2-x}\text{Sr}_x\text{CuO}_4$  (LSCO) system, SC and AF ordered phases are well separated: SC phase exists in a wide range of  $0.06 \leq x \leq 0.30$  and has a parabolic SC transition temperature,  $T_c$ , while AF phase is located in a narrow range of  $x \leq 0.02$ .<sup>3,4</sup> In contrast, in the electron-doped  $\text{Nd}_{2-x}\text{Ce}_x\text{CuO}_4$  (NCCO) and  $\text{Pr}_{2-x}\text{Ce}_x\text{CuO}_4$  (PCCO) systems, the optimum superconductivity adjoins a broad AF phase ( $0 \leq x \leq 0.14$ ) and the  $T_c$  decreases to zero in a narrow range ( $0.14 \leq x \leq 0.18$ ) as increasing  $x$ .<sup>5,6,7</sup> Therefore, it is important to clarify the origin of different doping symmetries and the essential features in the phase diagram.

On the other hand, recent intensive studies on the LSCO system by  $\mu$ SR<sup>10,11</sup>, nuclear magnetic resonance<sup>12</sup> and neutron scattering<sup>13</sup> techniques have claimed that a short-range AF ordered phase above  $x=0.02$  persists in under-doped regions up to  $x \sim 0.10$ , and therefore co-exists or phase separates with superconductivity. This penetration seems to contrastive feature with a competitive relation between AF and SC phases in the electron-doped systems, suggested in the aforementioned phase diagram. The universal phase diagram, however, is still controversial due to the limited number of comprehensive studies on both magnetism and superconductivity in the electron-doped system, and the difficulties in preparing samples, especially single crystals.<sup>14</sup>

In this paper, we present the phase diagram of the electron-doped PLCCO system<sup>15</sup> over a wide Ce concentration range using ZF- $\mu$ SR and magnetic susceptibility measurements. An advantage of this system is that the SC phase is extended to a lower doping region compared

to the PCCO system.<sup>8,9</sup> Thus, by investigating the magnetic phase in the system the relation between AF and SC phases can be clarified. Furthermore, compared to the NCCO system, a considerably smaller effect of the rare-earth moment is suitable for studying the inherent nature of  $\text{Cu}^{2+}$  spins. This study using single crystals as well as powder samples yields important information: (i) Upon Ce doping the AF ordered phase is drastically suppressed at  $x \sim 0.09$  where the SC phase abruptly appears at the ground state, suggesting a distinct competition between the two phases, and (ii) The confirmed SC region of the PLCCO ( $0.09 \leq x \leq 0.20$ ) is extended to both lower and higher Ce concentrations by La substitution into the PCCO system.

Single crystals ( $x=0.08, 0.09, 0.11, 0.13, 0.15, 0.17, 0.18$  and  $0.20$ ) and powder samples ( $x=0.04, 0.06, 0.09$  and  $0.11$ ) are grown using a traveling-solvent floating-zone method and a solid-state reaction, respectively. In order to induce the superconductivity with removing the relative oxygen content,  $\delta$ , of 0.03-0.05 per unit formula from as-grown samples, all samples are carefully annealed under argon gas flow at 900-950 °C for  $\sim 10$  h and single crystals are subsequently annealed under  $\text{O}_2$  gas-flow at 500 °C for  $\sim 10$  h. For the characterization of samples, we examined the Ce content and the lattice constants of the grown samples by the inductively coupled plasma (ICP) spectrometer and the X-ray powder diffractometer, respectively. Evaluated Ce concentrations are approximately the same with  $x$  in the chemical formula. At room temperature both  $a$  and  $c$ -axis lattice constants ( $I4/mmm$  notation) are larger than those in PCCO<sup>16</sup>, and change monotonously with  $x$ . Details of the sample preparation and the characterization will be presented in a separate paper.<sup>17</sup>

In order to determine  $T_c$ , we measured the diamagnetic susceptibility by a superconducting quantum interference device magnetometer. Figures 1(a) and (b) show the susceptibility for the annealed powder and the single

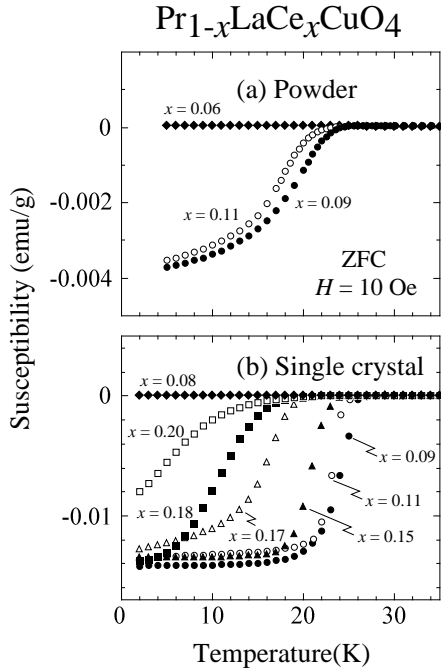


FIG. 1: Magnetic susceptibility measured for (a) powder and (b) single crystal samples of the PLCCO system.

crystal samples in an applied field of 10 Oe after the zero-field-cooling process. SC transitions are observed in the wide Ce concentration range of  $0.09 \leq x \leq 0.20$ , while there is not evidence for bulk superconductivity in the sample with  $0.08 \leq x$ . Based on these results the lower limit for the critical concentration of the bulk superconductivity is estimated to be between  $x=0.08$  and  $0.09$ . Note that the uniform magnetic susceptibility of PLCCO above  $T_c$  is only  $\sim 1\%$  of that of NCCO, demonstrating a qualitative edge of the PLCCO system for elucidation of magnetic properties of Cu spin.

$\mu$ SR measurements are performed on powder ( $x=0.04$ ,  $0.06$ ,  $0.09$  and  $0.11$ ) and single crystal ( $x=0.08$ ) samples at the pulsed muon source, RIKEN-RAL Muon Facility, Rutherford Appleton Laboratory in UK. These chosen values for  $x$  span the critical concentration. Positive surface-muons with perfectly polarized spins parallel to the beam and with the momentum of  $29.8$  MeV/c are implanted into sample. Then each muon stops and is depolarized by precessing around a local magnetic field at the muon site. Therefore, the time evolution of muon spin polarization ( $\mu$ SR time spectrum) obtained by the asymmetry of the decay positron emission rate between forward and backward counters,  $A(t)$ , provides information on the distribution and/or the fluctuation of the local magnetic field and the volume fraction of the magnetically ordered phase.<sup>18</sup>

In Fig. 2, the normalized  $\mu$ SR time spectra after subtracting time-independent background are shown for non-SC  $x=0.08$  and SC (b)  $x=0.09$  and (c)  $0.11$  samples. In all samples, a Gaussian de-

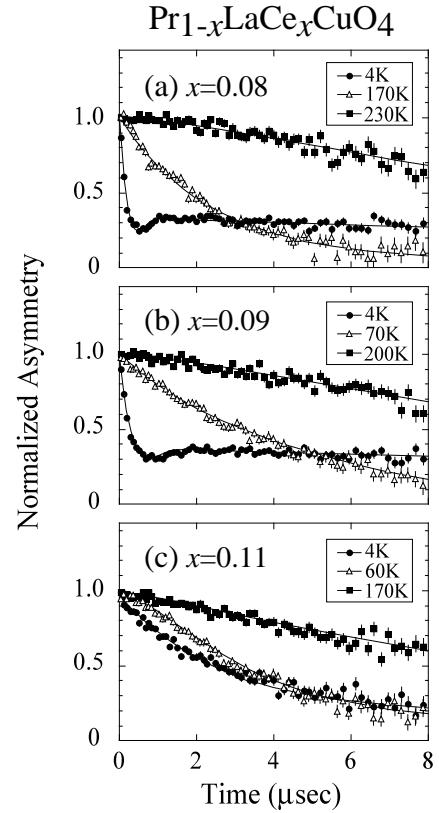


FIG. 2: ZF- $\mu$ SR time spectra of PLCCO with (a) non-superconducting  $x = 0.08$ , superconducting (b)  $0.09$ , and (c)  $0.11$ . Solid lines are results fitted with Eqs. (1) and (2). (See text.)

polarization is formed in the time spectra at high temperatures consistent with a static nuclear-dipole field and the rapid fluctuation of  $\text{Cu}^{2+}$  moments. At lower temperatures, the time spectra changes from a Gaussian-type depolarization to an exponential one. This change in the spectra suggests either the slowing down of  $\text{Cu}^{2+}$  spin fluctuation or formation of a somewhat disordered state like a spin-glass. Upon further cooling to  $4\text{K}$ , an additional muon spin rotation corresponding to the magnetic order appears in the  $x=0.08$  and  $0.09$  samples, while such a clear rotation is not observed in the  $x=0.11$  sample. Flat tail of the time spectra, suggesting the static order of Cu spins, is clearly seen because of a negligible effect of the Pr spin fluctuation. In contrast, contribution of the Nd spin fluctuation obscures the signal from Cu spins in the NCCO system. We note that the time spectra for SC  $x=0.09$  is similar to that of non-SC  $x=0.08$  rather than SC  $x=0.11$ , similar to the case of NCCO.<sup>19,20</sup> However, because of reduced effect from rear-earth moment, it is revealed that the magnetic properties of Cu spins change on accrossing the boundary, as shown next.

For the qualitative analysis of the time spectra, we first assumed a combination of Gaussian and exponential

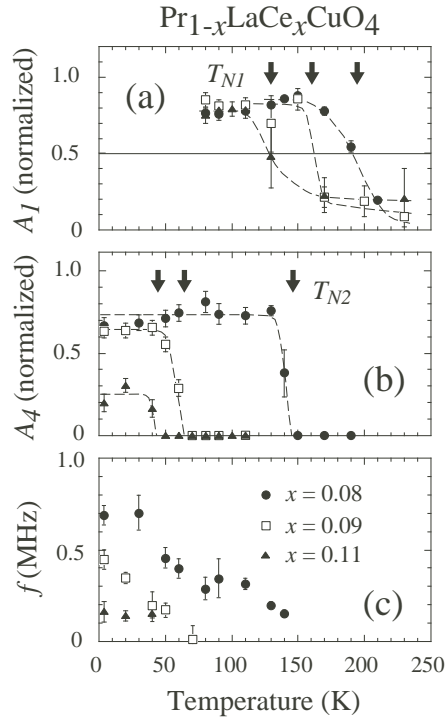


FIG. 3: Fitting parameters of (a) initial asymmetry  $A_1$  of the exponential component in Eq. (1), (b)  $A_2$  and (c) the frequency  $f$  of the rotation component in Eq. (2) for  $x = 0.08$ , 0.09 and 0.11 samples. Dashed lines are guides to the eye.

functions:

$$A(t) = A_1 \exp(-\lambda_1 t) + A_2 \exp(-\lambda_2 t^2), \quad (1)$$

with  $A_1 + A_2 = 1$ , where  $A_1$  and  $\lambda_1$ ,  $A_2$  and  $\lambda_2$  are the initial asymmetry at  $t=0$  and the depolarization rate for the exponential and Gaussian components, respectively. The time spectra at the higher temperatures ( $\geq 80$  K) are well reproduced by this function. The fitted results for the highest temperature are shown by solid lines in Fig. 2(a)-(c).  $A_1$  increases as the temperature decreases as shown in Fig. 3(a), then we defined characteristic temperatures as  $T_{N1}$  where  $A_1$  exceeds 0.5 or the exponential component dominates in the time spectra. To get more information regarding the ordered phase at low temperatures, the time spectra below  $T_{N1}$  were again fitted to the following equation:

$$A(t) = A_3 \exp(-\lambda_3 t) + A_4 \exp(-\lambda_4 t) \cos(2\pi ft + \phi), \quad (2)$$

with  $A_3 + A_4 = 1$ , where the first and second terms express components of relaxation and rotation of muon spin. The parameters  $A_3$  and  $\lambda_3$  are the initial asymmetry and the depolarization rate of exponential relaxation, respectively.  $A_4$  and  $\lambda_4$  are those of rotation component and  $f$  and  $\phi$  are the frequency and the initial phase of rotation, respectively. Solid lines for the time spectra at lower two temperatures in Figs. 2(a)-(c) are the fitted results from Eq. (2).

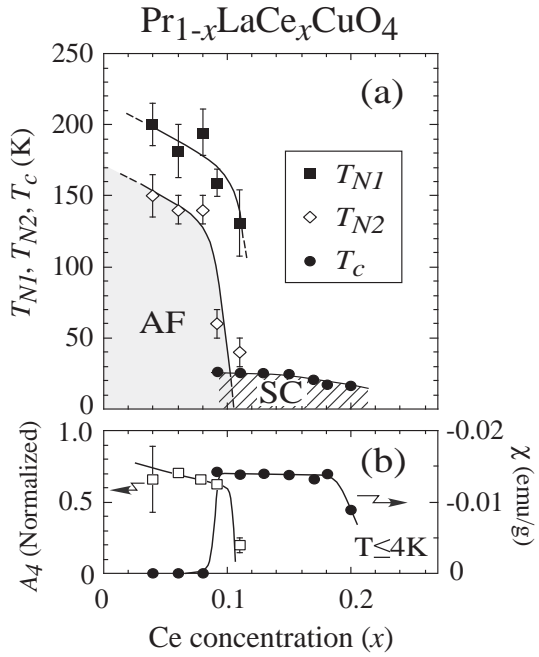


FIG. 4: Doping dependence of (a)  $T_{N1}$  (closed squares),  $T_{N2}$  (open diamonds) and  $T_c$  (onset) (closed circles) and (b) initial asymmetry for the rotation component of  $A_4$  (open squares) and diamagnetic susceptibility (closed circles) at temperature below 4 K. Solid lines are guides to the eye. Shaded and hatched areas in the upper figure correspond to AF ordered and SC phases, respectively.

In Figs. 3(b) and (c), the obtained parameters of  $A_4$  and  $f$ , that represent the AF volume fraction and the relative internal magnetic field at the muon site, respectively, are shown for the sample with  $x=0.08$ , 0.09 and 0.11.  $T_{N2}$  represents the onset temperature for the appearance of muon spin rotation. We note that there is no clear evidence of a static internal field for the temperature between  $T_{N1}$  and  $T_{N2}$  as the results were reported by Kubo *et al.*<sup>21</sup> This result suggests that in this temperature range the  $\text{Cu}^{2+}$  spins are fluctuating slower compared to the time scale of  $\mu\text{SR}$  measurement (typically  $10^{-6}$ - $10^{-11}$  sec) and there is a non-disordered state. Therefore, a *static* AF ordered state is recognized below  $T_{N2}$  in the  $\mu\text{SR}$  measurement. However, fluctuations above  $T_{N2}$  do not simply imply the absence of Néel state, defined as a state that has a *time-averaged* ordered moment. Indeed, magnetic Bragg peaks reflecting the time-averaged ordered moment are observed by elastic neutron-scattering measurements below about  $T_{N1}$ .<sup>22</sup> At low temperature as  $x$  increases, both  $A_4$  and  $f$  decrease. This correlates with the reduction of  $T_{N2}$ , indicating an uncertainty of AF ordered state upon electron doping. Furthermore,  $x$ -dependent  $f$ , suggesting a distinction of a coherent long-range ordered state, is different from the  $x$ -independent  $f$  in the LSCO system with  $x \leq 0.02$ <sup>23,24</sup> where the evidence of a phase separation between Néel state and spin-glass phase was observed.<sup>25,26</sup>

In Fig. 4 (a), the doping dependence of  $T_{N1}$ ,  $T_{N2}$  and  $T_c$ (onset) are summarized. Upon electron doping, bulk superconductivity with optimum  $T_c$  of 26 K abruptly appears at  $x \sim 0.09$  like a first order-transition and  $T_{N2}$  is dramatically suppressed at the same time. Therefore, at the ground state, SC phase appears with linking the disappearance of the AF ordered phase as seen in the NCCO system,<sup>7,19</sup> although two phases are partially overlapped due to coexistence or microscopically phase separation. This result combined with a relation between the doping dependences of  $A_4$  and the diamagnetic susceptibility,  $\chi$ , at low temperatures (Fig. 4(b)) clearly demonstrates a competitive relation between AF and SC phases. Such a relation is quite different from the results in the hole-doped system that show a penetration of short-range AF ordered phase into the under-doped SC one.<sup>10,11,12,13</sup>

Now we turn to the wide doping range of SC phase. As seen in Figs. 1(b) and 4(b), sharp SC transitions were observed for samples with  $0.09 \leq x \leq 0.15$  and the  $\chi$ 's at 2 K are constant, suggesting the appearance of homogeneous and bulk superconductivity. Therefore,  $T_c$  is certainly insensitive to the Ce concentration and this feature characterizes the wide SC phase, in contrast to previously obtained results for powdered samples. The expansion of SC phase would be related with the increase of metallic carriers by La substitution suggested from resistivity measurements.<sup>8</sup> Arima *et al.* reported a reduction of charge-transfer (CT) energy between Cu 3d and O 2p bands as stretching Cu-O bond, *i. e.*, lattice spacing.<sup>27</sup> If the reduction of the CT energy is greater than the loss from decreasing orbital overlap<sup>28</sup>, then the gain in mobility would make the introduction of electrons into the CuO<sub>2</sub> plane by La-substitution easier, resulting in the wider SC phase. In other words, the narrow SC phases in the NCCO and PCCO systems originate from the short lattice spacing. We note that SC phase of epitaxially grown PCCO thin film is analogously wider than that

of the powder sample at higher Ce-doped regions.<sup>29,30</sup> Nevertheless the SC phase of present PLCCO system is wider than that reported for PCCO thin film. On the other hand, for the appearance of superconductivity in the 2-1-4 electron-doped systems, a reduction procedure such as heat treatment is necessary. The role and effect of the reduction procedure, however, are not fully understood and inadequate treatment easily causes a reduction of  $T_c$ .<sup>14</sup> In order to clarify the fundamental features in electron doped superconductivity, further comprehensive studies on single crystals are required.

In conclusion, we have performed  $\mu$ SR and magnetic susceptibility measurements for the electron-doped PLCCO system. AF order was observed in the sample with  $0.04 \leq x \leq 0.11$ . The AF order was dramatically suppressed at  $x \sim 0.09$  which corresponds to the onset of the significantly wide SC phase ( $0.09 \leq x \leq 0.20$ ) upon doping. The obtained phase diagram combined with the doping dependences of AF volume fraction and internal magnetic field clearly demonstrates a competitive relation between AF and SC phases.

We thank M. Kofu and K. Hirota for technical assistance of ICP measurements at Tohoku University, and G-q. Zheng and K. Isawa for helpful discussion. This work was supported in part by the Japanese Ministry of Education, Culture, Sports, Science and Technology, Grant-in-Aid for Scientific Research on Priority Areas (Novel Quantum Phenomena in Transition Metal Oxides), 12046239, 2000, for Scientific Research (A), 10304026, 2000, for Encouragement of Young Scientists, 13740216, 2001 and for Creative Scientific Research (13NP0201) "Collaboratory on Electron Correlations - Toward a New Research Network between Physics and Chemistry -", by the Japan Science and Technology Corporation, the Core Research for Evolutional Science and Technology Project (CREST).

\* Electronic address: fujita@scl.kyoto-u.ac.jp

- <sup>1</sup> J. G. Bednorz and K. A. Müller, Z. Phys. B **64**, 189 (1986).
- <sup>2</sup> Y. Tokura, H. Takagi, and S. Uchida, Nature **337**, 345 (1989).
- <sup>3</sup> H. Takagi *et al.*, Phys. Rev. B, **40**, 2254 (1989).
- <sup>4</sup> J. B. Torrance *et al.*, Phys. Rev. Lett. **61**, 1127 (1988).
- <sup>5</sup> H. Takagi, S. Uchida, and Y. Tokura, Phys. Rev. Lett **62**, 1197 (1989).
- <sup>6</sup> G.M. Luke *et al.*, Nature **338**, 49 (1989).
- <sup>7</sup> G. M. Luke *et al.*, Phys. Rev. B **42**, 7981 (1990).
- <sup>8</sup> Y. Koike *et al.*, Jpn. J. Appl. Phys. **31**, 2721 (1992).
- <sup>9</sup> J. L. García-Muñoz *et al.*, Physica C **268**, 173 (1996).
- <sup>10</sup> A. Weidinger *et al.*, Phys. Rev. Lett. **62**, 102 (1989).
- <sup>11</sup> Ch. Niedermayer *et al.*, Phys. Rev. Lett. **80**, 3843 (1998).
- <sup>12</sup> M. -H. Julien *et al.*, Phys. Rev. B **63**, 144508 (2001).
- <sup>13</sup> M. Fujita *et al.*, Phys. Rev. B **65**, 064505 (2002).
- <sup>14</sup> K. Kurahashi, H. Matsushita, M. Fujita, and K. Yamada, J. Phys. Soc. Jpn. (to be published).
- <sup>15</sup> K. Isawa, M. Nagano, M. Fujita, and K. Yamada, Physica C, (to be published).

<sup>16</sup> For instance, *a* and *c*-axis lattice constants measured using an identical experimental setup are 3.986 and 12.304 Å for Pr<sub>0.85</sub>LaCe<sub>0.15</sub>CuO<sub>4</sub>, and 3.960 and 12.150 Å for Pr<sub>1.85</sub>Ce<sub>0.15</sub>CuO<sub>4</sub>.

<sup>17</sup> M. Fujita, unpublished data.

<sup>18</sup> R. S. Hayano *et al.*, Phys. Rev. B **20**, 850 (1979).

<sup>19</sup> T. Uefuji *et al.*, Physica C **357-360**, 208 (2001).

<sup>20</sup> I. Watanabe *et al.*, Physica C **357-360**, 212 (2001).

<sup>21</sup> T. Kubo *et al.*, Physica C, (to be published).

<sup>22</sup> M. Fujita, unpublished data.

<sup>23</sup> D. R. Harshman *et al.*, Phys. Rev. B **38**, 852 (1988).

<sup>24</sup> F. Borsa *et al.*, Phys. Rev. B **52**, 7334 (1995).

<sup>25</sup> F. C. Chou *et al.*, Phys. Rev. Lett. **71**, 2323 (1993).

<sup>26</sup> M. Matsuda *et al.*, cond-mat/0111228 (unpublished).

<sup>27</sup> T. Arima *et al.*, Phys. Rev. B **44**, 917 (1991).

<sup>28</sup> A. Manthiram, J. Solid State Chem. **100**, 383 (1992).

<sup>29</sup> J. L. Peng *et al.*, Phys. Rev. B **55**, R6145 (1997).

<sup>30</sup> P. Fournier *et al.*, Phys. Rev. Lett. **81**, 4720 (1998).